ELSEVIER

Chemical Geology 188 (2002) 105–123

CHEMICAL GEOLOGY
INCLUDING
ISOTOPE GEOSCIENCE

www.elsevier.com/locate/chemgeo

Carbon and nitrogen isotope systematics within a sector-growth diamond from the Mir kimberlite, Yakutia

G.P. Bulanova [a,b,*], D.G. Pearson [a], E.H. Hauri [c], B.J. Griffin [d]

[a] *Department of Geological Sciences, Durham University, South Road, Durham DH1 3LE, UK*
[b] *Diamond and Precious Metal Geology Institute, Siberian Branch, Russian Academy of Sciences, 39 Lenin Av., Yakutsk, Sakha Republic, Russia*
[c] *Department of Terrestrial Magnetism, Carnegie Institution of Washington, 5241 Broad Branch Road, N.W., Washington, DC 20015, USA*
[d] *Centre for Microscopy and Microanalysis, University of Western Australia, Nedlands 6907, Australia*

Received 29 March 2001; accepted 26 April 2002

Abstract

A single Yakutian octahedral diamond, displaying striking internal growth structure whereby cubic and octahedral growth sectors are inter-grown and surrounded by an octahedral rim, has been analysed for carbon and nitrogen isotopic compositions (by secondary ion mass spectrometry, SIMS), and for nitrogen concentration (by SIMS and Fourier transform infrared spectroscopy, FTIR) and nitrogen aggregation state (by FTIR). A graphite "seed" inclusion identified within the diamond is enriched in K, Ca, Ti, Rb, and Sr, providing evidence that the diamond may have grown from a carbonate melt/fluid interacting with upper mantle rocks. Carbon and nitrogen isotope compositions become progressively heavier from the core region ($\delta^{13}C = -7‰$ to $-5‰$ and $\delta^{15}N = -3‰$) towards the inner rim zones ($\delta^{13}C = -3‰$ and $\delta^{15}N = +8.9‰$ to $+5‰$) of the diamond. Nitrogen concentration and aggregation measurements show corresponding decreases that generally correlate with the isotopic variation. These systematic changes within the core and intermediate regions of the diamond are consistent with their formation during diamond growth from CO_2-rich fluids as a continuous event, accompanied by slight progressive isotopic fractionation of carbon and nitrogen. However, the observed isotope and nitrogen abundance trends differ from those predicted from thermodynamic modelling of fluid–solid equilibria in a C–N–O–H-bearing system due to changes in parameters such as f_{O_2}.Within the diamond octahedral rim region, grown by a layer by layer mechanism, nonsystematic variations in nitrogen abundance, nitrogen aggregation, and nitrogen and carbon isotope ratios were observed. Several interpretations are given for this phenomenon, including kinetic effects during growth of the diamond rim under different conditions from those of the core-intermediate regions; or rapidly changing fluid sources during the growth; or post-growth processes of nitrogen aggregation. No fractionation of nitrogen isotopes between cubic and octahedral growth zones was identified within the diamond, in contrast to the fractionation phenomena found in synthetic diamonds of mixed growth. Our results illustrate the potential C–N isotopic variation within individual diamonds and highlight the need for more studies of this type if the origin of isotopic variations in diamond suites is to be understood.

Keywords: Kimberlite; Diamond; Isotopes; Carbon; Nitrogen

* Corresponding author. 10 Upper Camden Place, BA1 5HX Bath, UK. Tel.: +44-1225-481588; fax: +44-1225-318550.
E-mail addresses: galina_bulanova@hotmail.com (G.P. Bulanova), g.pearson@durham.ac.uk (D.G. Pearson), hauri@dtm.ciw.edu (E.H. Hauri), bjg@cyllene.uwa.edu.au (B.J. Griffin).

0009-2541/02/$ - see front matter © 2002 Elsevier Science B.V. All rights reserved.
PII: S0009-2541(02)00075-X

1. Introduction and aims

The carbon and nitrogen isotope compositions of diamonds offer great potential in determining the source of carbon and the types of media from which diamonds grow (Deines, 1980; Galimov, 1984). However, despite a wealth of data, strong disagreements persist about both these factors. The controversy centres around the origin of the large isotopic variability of the global diamond database; $\delta^{13}C$ varies over 38‰, $\delta^{15}N$ varies over 34‰.

Deines (1980) and Javoy (1997) have suggested that this global isotopic variability of diamonds is a result of heterogeneities in the primordial carbon and nitrogen from which the diamonds grew. In contrast, Galimov (1991), Javoy et al. (1986) and Cartigny et al. (1998a,b) have argued that isotopic fractionation during growth is the dominant process producing isotopic variability between different diamonds. Others who believe in diamond origin via recycling of crustal carbon (e.g., Kirkley et al., 1991; Navon, 1999) relate the isotopic spectrum of diamonds to the variability of recycled material and mixing processes during subduction.

The traditional approach to the isotopic analysis of diamonds is to perform bulk analyses of individual diamonds. While this approach has provided much valuable data, it is limited in terms of not characterising potential isotopic variation within individual diamonds that may reveal processes occurring during their growth. With some exceptions (Javoy et al., 1984; van Heerden, 1993), most investigations of isotopic variation within diamonds have focussed on "coated" diamonds (Swart et al., 1983; Boyd et al., 1987, 1992). The regular octahedral cores and surrounding fibrous coats of coated diamonds represent extreme examples of different mechanisms and environments of their growth. The differences of 4‰ in carbon isotope composition found between core and coat have been interpreted as the result of Rayleigh distillation (Swart et al., 1983) or fractionation of carbon isotopes during growth (Galimov, 1984). Much more striking isotopic variations in nitrogen have been observed for differing crystallographic growth zones (cubic versus octahedral) in synthetic diamonds (Boyd et al., 1988). In spite of the different mechanisms of growth for cubic zones in synthetic and natural diamonds (Pal'yanov et al., 1997), it is still unclear whether such large-magnitude, growth-induced isotope fractionations can take place in nature between octahedral and cubic zones. To investigate these possibilities, detailed studies of the C and N isotopic variations within individual diamonds with respect to their growth forms, age, and crystallography are needed.

Recently, relatively precise in-situ measurement techniques using secondary ion mass spectrometry (SIMS) have been developed for carbon (Wilding and Harte, 1990; Harte and Otter, 1992; Harte et al., 1999; Fitzsimons et al., 1999) and also for combined carbon plus nitrogen isotope measurements (Hauri et al., 1999, in press). These developments offer great potential for improving our understanding of the causes of carbon and nitrogen isotope variations in diamonds, and hence providing better constraints on diamond origin, growth, and evolution.

Studies of Yakutian diamonds have revealed a great variety of internal growth morphologies between individual diamonds and also within single diamonds (Bulanova, 1995). This variation may be a reflection of changing environments during growth and hence makes the samples attractive targets for in-situ isotopic measurement (Hauri et al., 1999). In this paper we have focussed on a detailed, integrated study of a single diamond from the Mir kimberlite pipe, Yakutia, that displays stunning cubo-octahedral sectorial zonation. This internal growth zonation provides an ideal opportunity to investigate potential crystallographic controls on carbon and nitrogen isotope variation in the light of the variation observed within a synthetic diamond by Boyd et al. (1988). The diamond we have studied, 1137, has been characterised using cathodoluminescence (CL), FTIR and SIMS. These techniques allow nondestructive, in-situ characterisation of the diamond at the 10- to 30-μm scale of lateral spatial resolution. The ability of both FTIR and SIMS techniques to determine N abundances allows a comparison of measurements using these methods which sample greatly different integrated depth-scales. A preliminary FTIR study of this specimen has been made by Griffin et al. (1995) and photoluminescence observations have been reported by Beskrovanov (1992).

2. Diamond external and internal morphology

Diamond 1137 from the Mir kimberlite pipe, Yakutia, is a colourless step-layered octahedron of 2-mm diameter, containing a black central inclusion. Birefringence (BR) and photoluminescence imaging of the whole diamond display an excellent example of sectorial cubo-octahedral growth in the central and intermediate regions succeeded by simple octahedral growth in the rim zone. The unusual internal structure of the stone was revealed even more clearly in a central "plate" made by mechanical polishing through the centre of the diamond, the resultant "plate" being slightly inclined to the dodecahedral plane (Fig. 1). CL images of both sides of the plate are not identical, indicating that the central position of the zoned sectorial structure is closer to one side of the plate (Fig. 1a) than the other (Fig. 1b). In the central section of the diamond parallel to (110), the octahedral growth zones are essentially orthogonal to the plate surfaces and coherent through the plate for the Infra Red measurements (Fig. 1a). Compared with the octahedral growth zones, the cubic sectors have more complicated positions: two lobes located along the long diagonal of the plate are approximately orthogonal to the surface of plate, but they have no manifestation on the other side of the relatively thick plate. Two other cubic sectors located along the small diagonal are inclined at 45° to the surface of both sides of the diamond plate (Fig. 1a,b). Three main regions of the diamond are defined as described below, within which additional fine structures can be discerned.

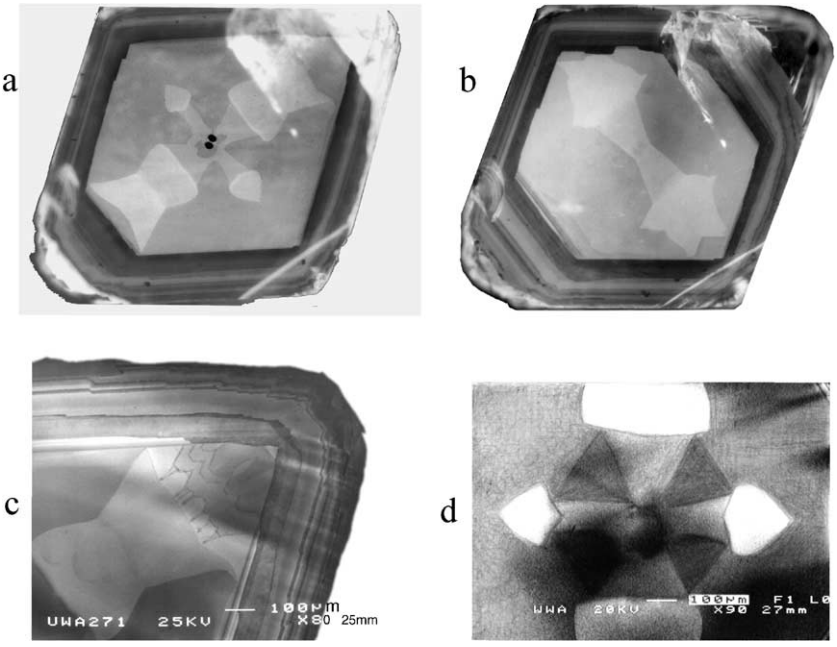

Fig. 1. (a) Cathodoluminescence (CL) image of central plate of Mir diamond 1137 polished along a dodecahedral plane. The central region has a cubo-octahedroidal shape (light-grey cubic lobes and dark-grey octahedral sectors on the image). The intermediate region consists of cubic sectors (white on photo) and octahedral zones (dark grey on the photo); the rim area is composed of octahedral zones (black peripheral zone with narrow grey zone inside). Two black spots in the centre are marks on the diamond surface from ion microprobe beam; magnification × 40. (b) CL image of the other side of the 1137 diamond plate. Cubic sectors are revealed only along the short diagonal of the plate; the same magnification. (c) SEM CL image of saw-tooth-like texture in the right upper octahedral corner of diamond plate 1137 (see Fig. 1a). The texture appears as an interpenetrating structure along the cuboidal surface and during the next stage of growth these "negative pits" covering the cubic faces developed into pyramidal-shaped ones; magnification × 80. (d) SEM CL image of the core region of diamond 1137 showing details of the central cross structure. The boundary of the octahedral zones (ends of the four dark-grey sectors) are flat, but cubic "paleo-faces" (ends of the four light-grey sectors) display a negative relief in agreement with their mechanism of growth; magnification × 90.

2.1. Core region

A crystallographically complex diamond core 550 μm across surrounds a black central inclusion (Figs. 1d and 2) and is composed of cubic and octahedral sectors in almost equal proportions with the growth rate of cubic sectors slightly decreased. The resulting shape of growth of the core region is an isometric cubo-octahedron, formed by layered octahedral zones showing blue CL and hummocky cubic lobes with weak green-blue CL. Thus, the mechanism of growth of the core inner zone was mixed: faceted (layer by layer) for octahedral zones and unfaceted (hummocky) for cubic sectors (Moore and Lang, 1972). The interfaces of the octahedral zones are flat and smooth. The paleo-faces defining the cubic sectors are not flat but are crystallographic surfaces displaying negative relief with hummocky surfaces because each cuboid face has only an average orientation in a cube direction (Moore, 1985; Fig. 1d). Therefore, it is more fitting to use the term cuboido-octahedron for this core diamond region.

2.1.1. Central inclusion—"seed"

The location of a black inclusion (50-μm width) exactly in the growth centre of the crystal suggests that it was a seed-mineral for diamond nucleation, which is a common feature of Yakutian diamonds (Varshavsky, 1968). Electron microprobe analysis with the beam focused under the surface failed to detect the presence of any major element, indicating that this inclusion is almost certainly graphite. The frequent presence of graphite as a central inclusion in Yakutian diamonds has been shown by Bulanova et al. (1986) and Bulanova (1995).

Various observations have shown that such type of graphite is primary and not a product of late-stage graphitisation of the host diamond. The shape of the graphites (hexagonal plates) and their common position exactly in the growth centre of the host diamonds indicate their syn- or even protogenetic nature and their seed role for diamond nucleation. X-ray microdiffraction of these central graphite inclusions reveal them to be of monocrystalline structure (Bulanova et al., 1979), in contrast with the polycrystalline epigenetic graphite aggregates developed in diamond cracks during the late graphitisation processes. Proton-microprobe analysis of the central inclusion in 1137 (also focusing the beam into the inclusion below the surface) showed a significant amount of K, Ca, Ti, Cr, Fe, Ni, Rb, and Sr (Bulanova et al., 1998). It is unclear whether these elements are impurities in the graphite matrix or are separate micro-phases. High abundances of K, Ca, Ti, Rb, and Sr are typically associated with carbonate melt/fluid and the presence of such melt (fluid) has been identified as a component of inclusion-seeds in many diamonds from Yakutian kimberlites (Bulanova et al., 1986, 1998).

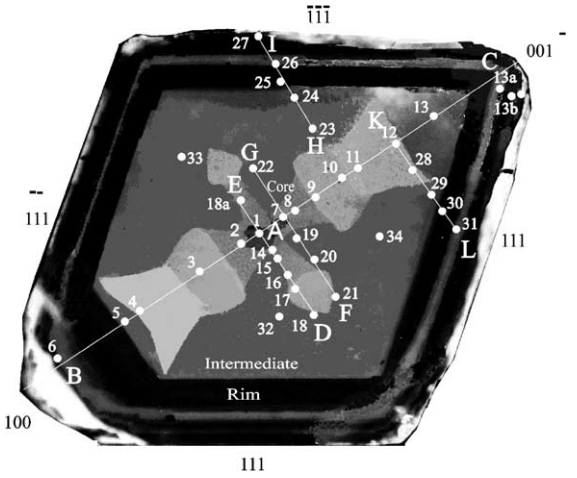

Fig. 2. Computer-enhanced CL image of 1137 central diamond plate slightly repolished after FTIR measurements. The rim zone is revealed in the upper right corner. Three main growth regions, crystallographic directions and lines of traverses made by SIMS measurements are shown; magnification × 60.

2.2. Intermediate region

The growth shape of the intermediate region (width 500 μm) is also cuboido-octahedral (Figs. 1a and 2) and its growth mechanism was mixed, as for the central region. Octahedral zones have the same blue CL colour, but cubic lobes show a bright yellow-green CL colour. The rapid change of growth rate in the cubic zones is documented by their sharply variable widths (Figs. 1a and 2). The size of the cubic sectors doubles, indicating a sudden slowing of growth rate, most probably caused by selectively absorbed impurities.

During the last stages of growth of the intermediate zone, the morphology changed from cuboido-octahedral to octahedral. The mechanism of this transforma-

tion is documented clearly by a peculiar texture in one corner of the cubic sector, as revealed by scanning electron microscopy (SEM) CL imaging (Fig. 1c). The texture appears as an interpenetrating structure along the cuboidal surfaces, producing a saw-tooth-like profile on the cubic interfaces. During the next stage of growth, these "negative pits" covering the cubic faces developed into pyramidal-shaped ones (Fig. 1c). Following this transition, diamond growth was dominated by planar, faceted growth. Negative pits along the cuboidal surfaces of diamonds, grown by a mixed mechanism, are described by Suzuki and Lang (1976). They proposed that they are located on the exits of dislocations, reflected by development within the pits of a cell structure ("cobble-stone pavement" type). In diamond 1137 this structure is revealed as the saw-tooth-like profile of Fig. 1c, closely associated with narrow bright-yellow CL zones.

2.3. Rim region

The rim region, of 170-μm thickness, is composed of thin octahedral layers that exhibit no CL colour apart from a few, very narrow, blue zones in the middle (Figs. 1 and 2). This diamond region was formed by a layer-by-layer mechanism of growth similar to that commonly seen in other Yakutian diamonds.

3. Analytical techniques

FTIR measurements were collected over the whole plate on a 200-μm spaced 22×22 point grid. These data have been individually reduced to yield nitrogen concentration and hydrogen peak area (at 1137 cm^{-1}) data and aggregation temperatures, following the methods described by Taylor et al. (1990), Taylor et al. (1996), and Mendelssohn and Milledge (1995). For determination of the 1aA nitrogen content an absorption coefficient of 160 at. ppm was used. A value of 750 at. ppm/mm has been used as the coefficient for IaB aggregated nitrogen. This value was selected from the range of 650–1000 at. ppm/mm given by Mendelssohn and Milledge (1995). Use of these differing values gives a difference of only 5 °C for calculated mantle residence times.

N abundance and C and N isotope ratios were measured for the diamond plate in situ via secondary ion mass spectrometry (SIMS) using a Cameca IMS 6f ion microprobe (Hauri et al., 1999, in press). With sufficient care given to instrument alignment and standardisation, $\delta^{13}C$ in diamond can be determined to $\pm 0.6‰$ (2σ) total uncertainty (comprising $\pm 0.4‰$ analytical precision plus $\pm 0.2‰$ accuracy from standards). All measurements were performed with the standard and sample mounted in the same analytical block to optimise performance. Reproducibility of $\delta^{15}N$ measurements can be as accurate as $\pm 2‰$ depending on N abundance, but standard heterogeneity currently limits the accuracy of $\delta^{15}N$ data to $\pm 6‰$ (2σ). For individual sample traverses, it should be possible to resolve 2‰ relative variation in N isotopic composition. Nitrogen abundance measurements, obtained during $\delta^{15}N$ measurements, have an accuracy of $\pm 10\%$ and a detection limit of 0.5 ppm by weight. Detailed discussion of instrumental techniques are given in Hauri et al. (1999, in press).

The multi-technique nature of this study allows comparison of nitrogen abundance measurements by SIMS and FTIR. It should be borne in mind that the spatial resolution used for SIMS is finer than for FTIR and that the vertical sampling scales of the FTIR and SIMS measurements are vastly different. The FTIR response is integrated from the entire thickness of the diamond plate whereas the depth sampled by the ion-microprobe beam is of the order of a few microns maximum. For FTIR measurements, a given N abundance represents the average of several growth zones, which may have widely different N content and could be measured individually only by SIMS (Harte et al., 1999). Analyses sites for SIMS nitrogen measurements, where fine-scale zoning was evident during ion-imaging by SIMS, were specifically chosen as high-N growth zones in order to give a maximum signal for isotopic measurements. In this way, the SIMS analytical sites were systematically different from those likely to have been sampled by FTIR.

Comparison of in-situ SIMS N concentration determinations with CL image brightness is complicated by uncertainty in the exact correlation of analytical locations for SIMS compared with the growth zones revealed by CL due to the inability to view the specimen in CL mode.

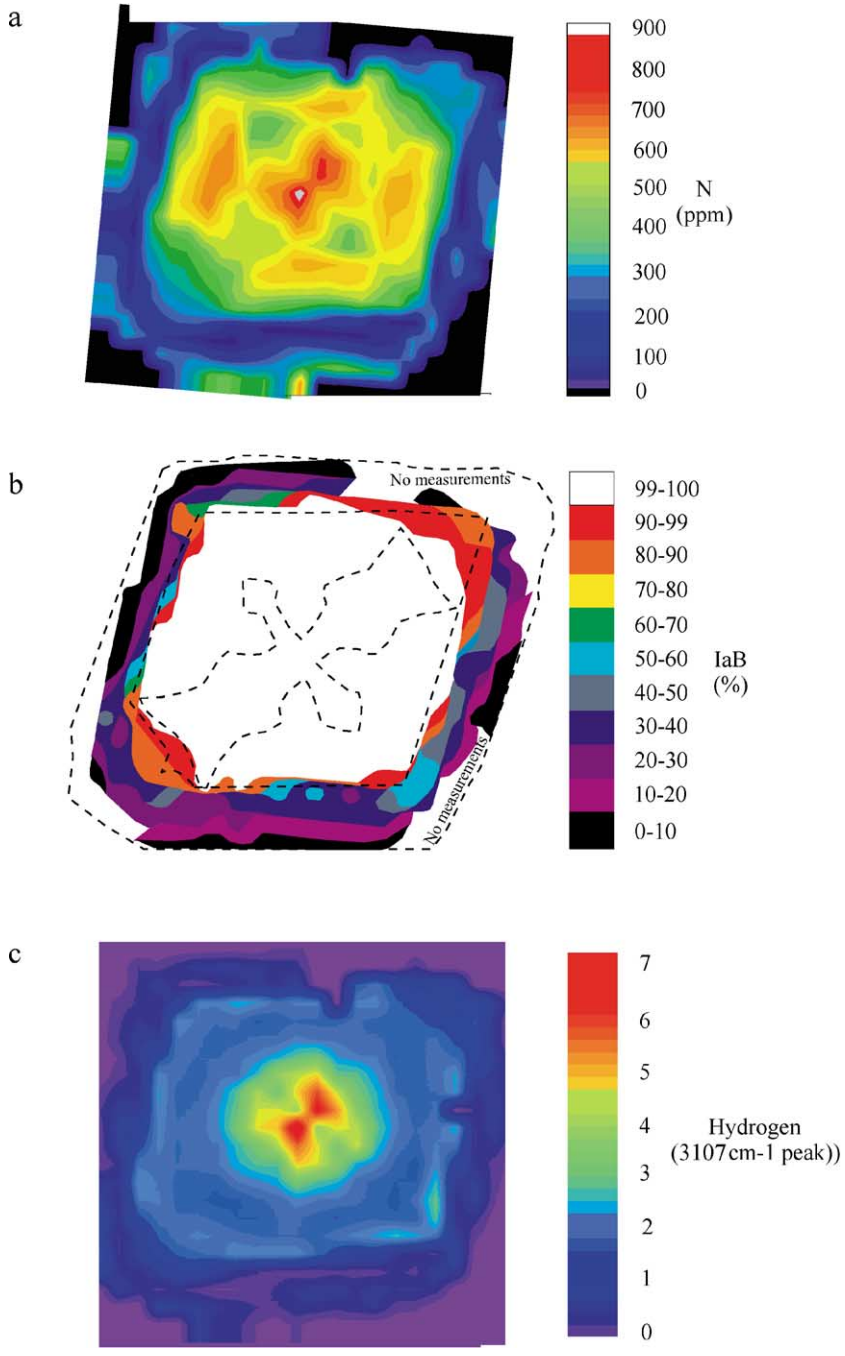

Fig. 3. Spatial distribution maps of nitrogen concentration, nitrogen aggregation state, and hydrogen concentration in diamond 1137 from FTIR data. (a) Distribution of nitrogen concentration (at. ppm). (b) Distribution of B-defect nitrogen; scale in percent of total nitrogen as type 1aB substitutional form; contours of central cross structure shown. (c) Relative hydrogen (3107 cm^{-1} peak) distribution.

4. Results

4.1. FTIR data: hydrogen and nitrogen abundance and distribution, aggregation of nitrogen

N abundance as measured by FTIR provides a good match with the internal structure of the 1137 diamond revealed by CL imaging. The core region has the highest nitrogen content at 900–750 at. ppm, which is virtually fully aggregated (close to pure type 1aB diamond) (Figs. 3a,b and 4). The cubic lobes of the central cross have slightly higher nitrogen content (900–850 at. ppm) relative to the octahedral sectors (800–750 at. ppm).

Hydrogen content is unusually high and its distribution follows the general pattern of nitrogen concentration (Fig. 3c), being highest in the core and lowest in the rim of the diamond. Within the core the highest hydrogen concentrations are within the cubic sectors, which also have the highest nitrogen concentrations. In the outer zone of the core, hydrogen abundance is lower and does not correlate with nitrogen variation and sectorial structure.

Nitrogen abundances in the intermediate region of the diamond are lower and relatively inhomogeneous. In contrast to the core region, the concentration of nitrogen in cubic lobes of the intermediate region is lower (600–500 at. ppm) than in octahedral zones (700 at. ppm), and generally decreases in both sectors towards the rim of the crystal. Aggregation of nitrogen within both cubic and octahedral sectors in the intermediate region is still very high as in the core area, i.e.,

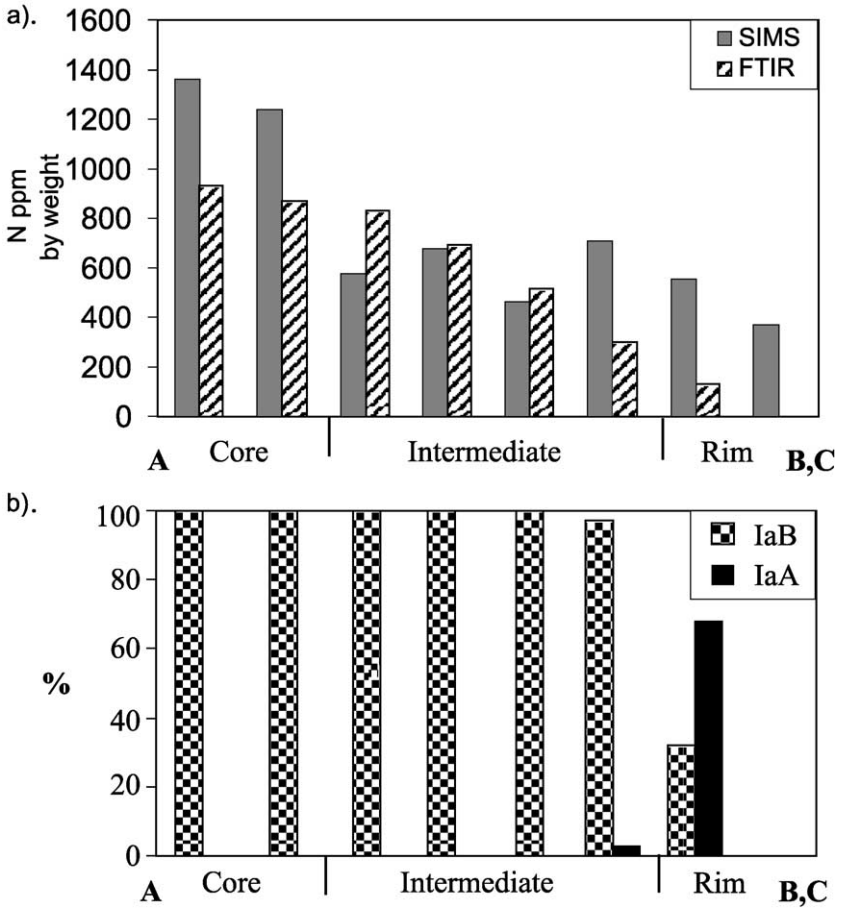

Fig. 4. Plots of traverses AB–AC made by SIMS and FTIR across plate 1137. (a) Comparison of SIMS and FTIR nitrogen concentration determinations, all data converted to ppm by weight. (b) Nitrogen aggregation state as determined by FTIR.

close to 100% 1aB type (Figs. 3b and 4b). The hydrogen content of the intermediate region is low.

The rim region of the diamond has a generally dark CL response and contains much lower levels of nitrogen than the core and intermediate regions (200–50 at. ppm). The rim region is also characterised by variable but low states of nitrogen aggregation (Figs. 3b and 4b). The rim region might consist of fine intergrowths of type I and type II diamond that are integrated by the FTIR signal but picked out by the finer sampling of the SIMS analysis. A narrow zone of blue CL colour contains moderate nitrogen concentration (200 at. ppm), which is mainly poorly aggregated (type IaA). Hydrogen contents (Fig. 3c) are low in the rim region.

4.2. SIMS data: nitrogen content, carbon and nitrogen isotope composition

Six SIMS traverses have been made across the diamond plate (Fig. 2). Two main traverses, AB and AC, across the core region of the cubic lobes of the plate (Fig. 2) contain a complete set of SIMS data (Table 1) and therefore are mostly used for interpretation. Traverse DE along the second pair of cubic sectors was made slightly off-centre and represents mainly $\delta^{13}C$ SIMS measurements. Traverses FG and HI cross the octahedral sectors (Table 1). Short traverse KL and a few other points shown on Fig. 2 were analysed for carbon isotope composition only (Table 1).

4.2.1. Correlation of N abundance and carbon isotopes

In general, high nitrogen concentrations correlate with the lightest carbon isotope compositions in the majority of the traverses across the 1137 sample. Traverse 'AB' (Fig. 2) crosses the first cubic sector of the long diagonal spanning the diamond plate. It displays a clear "centre-rim" trend with $\delta^{13}C$ increasing from $-5‰$ (core) to $-2.4‰$ (rim), and a corresponding decrease in nitrogen abundance by a factor of 3, from 1440 to 468 ppm by weight (Fig. 5a,b). The continuation of this "centre-rim" traverse along the second cubic sector ('AC' on Fig. 2) reveals a similar trend. It starts with $\delta^{13}C$ of $-4.1‰$ not far from the centre, fluctuates slightly in the intermediate zones and terminates with a $\delta^{13}C$ value of $-3.5‰$ in the rim region (Table 1, Fig. 5a,b). The SIMS measurement for the central region along the 'AC' traverse (point 7) was made slightly further from the centre of the diamond growth compared with point 1 along the 'AB' traverse. The measurements within the intermediate regions fluctuate slightly, but are in a good agreement for both 'AB' and 'AC' traverses (e.g., points 11 and 3), providing indirect support for the estimates of precision and accuracy.

The 'centre-rim' measurements were made also along the small diagonal of the plate ('DE' on Fig. 2; across the other pair of cubic sectors, inclined at 45° to the surface). This traverse does not show a distinctive trend in carbon isotope composition, although nitrogen contents decrease from the centre to the intermediate area of the diamond (Table 1). The position of these analytical points lies in an area of mixed growth forms (cubic + octahedral) and this could account for the lack of a clear trend for the carbon and nitrogen isotopes. Additionally, few measurements were taken along this traverse, and therefore there is a lack of data for the rim zones.

The other traverse via the core through the sectors of diamond composed by distinctive octahedral zones ('FG–HI' on Fig. 2) displays a clear increase in $\delta^{13}C$ with distance. It becomes heavier away from the core to the inner rim region, but reverts back to the isotopically light values within the outer rim (Table 1, Fig. 5d). From the core through the intermediate and inner rim zones, $\delta^{13}C$ increases from $-7‰$ to $-3.2‰$. Within the outer rim zone $\delta^{13}C$ is similar to that in the marginal parts of the diamond core ($-5.2‰$), which possibly could be explained by complex intergrowths of two different physical types of diamond here. N abundance decreases from the core towards the diamond rim within this octahedral sector of growth (Fig. 5c).

4.2.2. Nitrogen abundances and nitrogen isotopic compositions

In general, $\delta^{15}N$ values in diamond 1137 increase with decreasing N abundance, in agreement with other studies of variations within natural diamonds (Boyd et al., 1992). The overall variation in nitrogen isotope systematics shows the same general trend as for the carbon isotopes. $\delta^{15}N$ values vary from being relatively light in the core areas ($-3.6‰$) towards generally heavier values in the rim ($>1‰$, Fig. 5).

Table 1
Primary SIMS C–N isotope and N abundance data for diamond 1137

Traverse	Region	Points	$\delta^{13}C$ (‰)	$\delta^{15}N$ (‰)	N (ppm by weight)
AB via first cubic sector	core	1	− 5	− 2.5	1540
(long diagonal of plate)	core	1 repeat	n.a.	− 3.9	1340
	core	1 av.	− 5	− 3.2	1440
	core	2	− 4.2	− 1.9	1150
	intermediate	3	− 3.3	− 2.1	610
	intermediate	3 repeat	n.a.	− 2.7	713
	intermediate	3 av.	− 3.3	− 2.4	661
	intermediate	4	− 4.2	− 0.1	458
	end of intermediate	5	− 2.7	1.1	769
	rim	6	− 2.4	9.3	468
AC via second cubic sector	core	7	− 4.1	− 3.4	1290
(long diagonal of plate)	core	8	− 4.4	− 4	1320
	intermediate	9	− 3.8	− 3.1	576
	intermediate	10	− 3.4	− 2.9	676
	intermediate	11	− 3.4	− 2.9	696
	intermediate	12	− 4.4	− 4.3	463
	end of intermediate	13	− 3.2	− 3.3	645
	rim	13a	− 3.4	8.6	262
	rim	13b1	− 3.5	2.4	298
	rim	13b2	− 3.5	− 1.5	444
DE via third cubic sector	core	14	− 5.7	n.a.	n.a.
(short diagonal of plate)	core	15	− 5.7	− 3.8	1810
	core	16	− 3.5	n.a.	n.a.
	intermediate	17	− 3.1	− 3.6	736
	intermediate	18	− 5.6	n.a.	n.a.
	core	18a	− 3.7	− 3	707
FG via octahedral zones	core	19	− 7	− 3.9	1800
	core	19 repeat	n.a.	− 3.3	1890
	core	19 av.	− 7	− 3.6	1845
	core	20	− 5.4	n.a.	n.a.
	intermediate	21	− 4.6	n.a.	n.a.
	intermediate	22	− 4.8	n.a.	n.a.
HI via octahedral zones	core	23	− 4.4	n.a.	n.a.
	intermediate	24	− 4.3	− 2.1	561
	intermediate	25	− 3.2		806
	rim	26	− 5.6	5.3	459
	rim	27	− 5.2	− 3.9	788
KL via octahedral zones	intermediate	28	− 2.9	n.a.	n.a.
	end of intermediate	29	− 3.4	n.a.	n.a.
	rim	30	− 2.5	n.a.	n.a.
	rim	31	− 2.5	n.a.	n.a.
Other points	intermediate	32	− 3.4	− 3.2	1300
	intermediate	33	− 3.3	n.a.	n.a.
	intermediate	34	− 2.9	n.a.	n.a.

Analytical precision: ± 0.4 ‰ on $\delta^{13}C$, ± 2 ‰ on $\delta^{15}N$, and ± 1% ppm on N.
Total uncertainties (at 2σ): ± 0.6 ‰ on $\delta^{13}C$, ± 8 ‰ on $\delta^{15}N$, and ± 10% ppm on N.

Within this overall trend marked anomalies exist, such as point 6 of the 'AB' traverse, 13a of traverse 'AC', and 26 of traverse 'HI', which have highly positive $\delta^{15}N$ (+9.3 to +5.3 at. ppm, Table 1). Such extreme N-isotopic fluctuations may be a function of the complex intergrowth of type II diamond (dark in CL) and type I that characterises the rim region in this area. Such narrow, dark CL nitrogen-free zones of

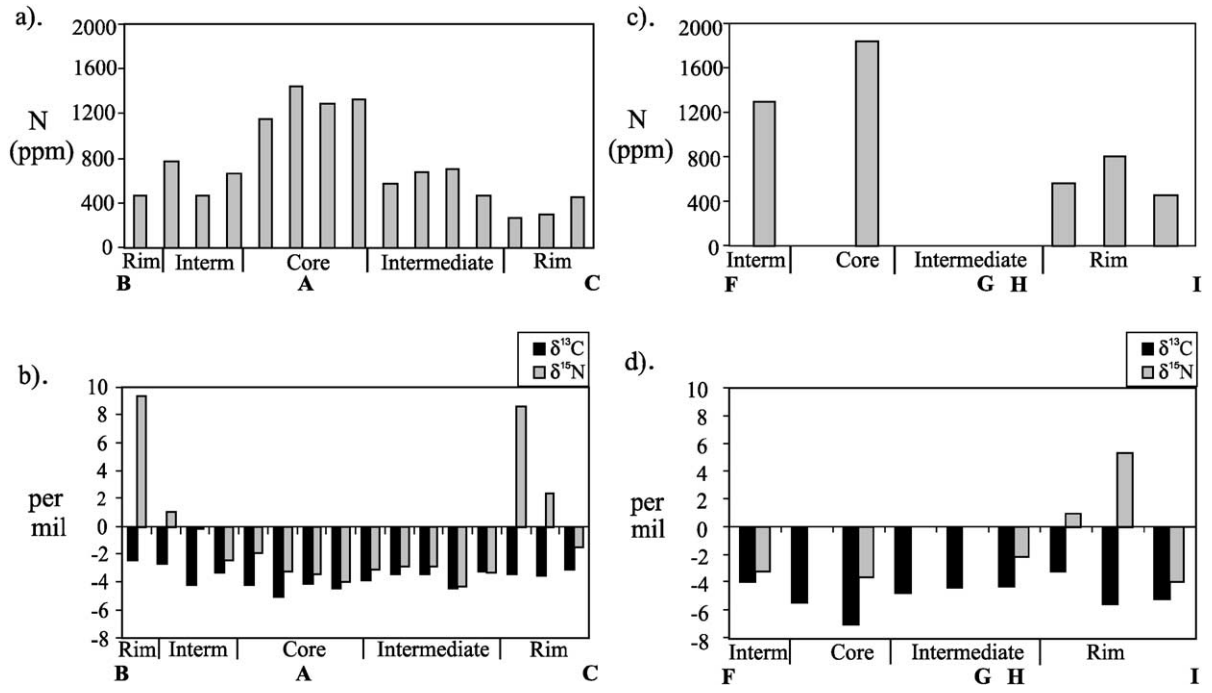

Fig. 5. Nitrogen isotopic composition and nitrogen abundance from SIMS in individual traverses via the core of plate 1137. (a) Nitrogen concentration distribution (ppm by weight) across AB–AC traverses. (b) Carbon and nitrogen isotope compositions for individual data points across AB–AC traverses. (c) Nitrogen concentration distribution (ppm by weight) across FG–HI traverses. (d) Carbon and nitrogen isotope compositional variation across the FG–HI traverses.

diamond are common within Yakutian diamonds where an abrupt change of growth shape took place. Similar characteristics are also regularly observed as local zones surrounding syngenetic inclusions (Bulanova, 1995).

5. Discussion

5.1. Time/temperature constraints from FTIR data

The aggregation of nitrogen within the diamond lattice is a function of both time and temperature (e.g., Evans and Harris, 1989; Taylor et al., 1990). If diamond residence in the mantle is greater than 200 Ma then the nitrogen aggregation state is relatively insensitive to time and is best used as a thermometer (summarised in Navon, 1999). Although effects such as plastic deformation, impurities, and variation in growth rates may have some effect on the aggregation of N in diamond (Taylor et al., 1996), these effects are not well constrained. For example, the highly aggregated Argyle diamonds have an abundance of deformation lamellae, however, there is not sufficient global evidence recorded as yet to evaluate this possibility systematically. These reservations notwithstanding, nitrogen aggregation can be used to place some useful constraints on the thermal history of diamonds. Here we use the approach of Taylor et al. (1990) to calculate the possible mantle residence temperature for sample 1137. Using a mantle residence time of c. 2.9 Ga, estimated from Re–Os dating of P-type sulphide inclusions in diamonds from the Udachnaya kimberlite, Yakutia (Pearson et al., 1999), aggregation temperatures for the well-aggregated central region of 1137 have a mean of approximately 1360 °C. The less aggregated rim region of 1137 gives a lower mean temperature of 1160 °C.

The simplest explanation for the observed variation in calculated mantle residence temperature from core to rim is likely to be that the rim is a later, second stage growth event that post-dated the formation of the Core-Intermediate regions. This option is consistent with the observed differences in carbon and nitrogen isotope compositions between these regions.

5.2. Isotope trends and nitrogen distribution

We have observed consistent changes in nitrogen content and nitrogen and carbon isotope composition that correlate with the internal structure of the diamond. The simplest explanation of these trends is that they are a reflection of varying conditions during the growth of this diamond. Therefore, it is important to consider average isotopic compositions of discrete crystallographic zones and sectors that are located symmetrically around the centre of crystal growth, so that we can examine general evolutionary trends for the whole diamond during its growth.

5.2.1. Nitrogen abundance: comparison of FTIR and SIMS results

Summarised FTIR and SIMS data for the main traverses are presented as averages of measurements within the same zones and growth sectors in Table 2 and on Fig. 4a. Despite the differences in the scale of depth sampling between FTIR measurements (full-plate width) and the ion-microprobe measurements (a few microns of surface), both results are in agreement in terms of showing the same general evolutionary trends. Nevertheless, when all the data are calculated using the same units, i.e., converting the FTIR abundances to ppm by weight from at. ppm, the absolute values of nitrogen from SIMS measurements in the core diamond zones are approximately 1.5 times higher than those from FTIR (Table 2, Fig. 4a). This difference can be explained by the combination of nonisometric internal zoning of the diamond and the large difference in vertical sampling scale of FTIR and SIMS.

The cubic zones along the long diagonal of the central diamond section are not manifested on the other side of the plate (Fig. 1a,b). Hence, an FTIR measurement of the highest N cubic sector shown on the central surface of the plate will also integrate and be diluted by the lower N octahedral sector below the surface. In contrast, measurement by SIMS of the top cubic sector will sample only the upper, highest in N cubic sector of the diamond. This situation will lead to a systematic bias towards higher N concentration values for the SIMS measurements as evident in Fig. 4a.

In other situations where a higher N content sector underlies an upper surface cut through a lower N content sector, the FTIR measurement will lead to higher N concentrations than the SIMS measurement, as in the case of the intermediate area of the diamond (Fig. 4a). Where different types of diamond are intergrown on a fine scale within the ‘‘saw-tooth’’ like texture corner of the diamond (points 5 and 13, Table 2, Fig. 2), SIMS measurements are grossly different from FTIR nitrogen abundance measurements.

Thus, for diamonds showing complex nonisometric cubo-octahedral growth zonation such as 1137, we would expect systematic biases to be evident between SIMS and FTIR N abundance measurements, depending on the regions of the crystal analysed. This complicates comparison of the two techniques.

A similar case was found by Harte et al. (1999) for several different Southern African diamonds. Because the SIMS measurement points sample individual growth zones, the SIMS results may be subject to more variability. It is also possible that additional N is present in non-centro symmetrical molecules that would not have an FTIR response. This possibility still needs investigation; there is no record in the literature of such studies. Despite these complications and discrepancies, comparison of FTIR and SIMS nitrogen abundance measurements of the sectorial diamond 1137 appears in better general agreement than for similar measurements made in the complex specimens studied by Harte et al. (1999).

5.2.2. Correlations: N abundance and aggregation—carbon and nitrogen isotopes

Previous in-situ studies of nitrogen and carbon isotope variation within noncoated diamonds have generally found little correlation between nitrogen content and carbon isotope composition (Harte and Otter, 1992; Harte et al., 1999; Fitzsimons et al., 1999). Some limited variations in carbon isotope compositions were recorded in specimens from Koffiefontein, South Africa (Harte et al., 1999), and George Creek, USA (Fitzsimons et al., 1999). Where variations do occur, they tend to be sharp, and occur across growth banding.

Table 2
Summary of isotope and N abundance (ppm by weight) data for diamond 1137

SIMS data									FTIR data		
Traverse	Average of points	Region	CL colour	Location	Shape	$\delta^{13}C$ (‰)	$\delta^{15}N$ (‰)	N (ppm)	N (ppm)	IaB (%)	IaA (%)
AB–AC (1–13a) across cubic sectors (long diagonal of plate)	1 and 7	core	green-blue	core-1 (inner)	cubo-octahedral	−4.55	−3.3	1365	928	100	0
	2 and 8	core	green-blue	core-2 (outer)	cubo-octahedral	−4.3	−2.95	1235	869	100	0
	9	intermediate	yellow	cubic lobes start	cubo-octahedral	−3.8	−3.1	576	828	100	0
	3, 10, 11	intermediate	yell.-green	cubic lobes mid.	cubo-octahedral	−3.4	−2.73	677	689	100	0
	4 and 12	intermediate	yell.-green	cubic lobes end	cubo-octahedral	−4.3	−2.2	460	512	100	0
	5 and 13	end of intermediate	blue	"saw-tooth" corner	octahedral	−2.9	−1.1	707	302	97	3
	6 and 13a	rim	blue	rim-2 (2d. inner)	octahedral	−2.9	8.95	556	127	32	68
	13b1, 13b2	rim	dark	rim-3 (outer)	octahedral	−3.3	0.5	371	0	n.a.	n.a.
DE (14–18) across cubic sectors (short diagonal of the plate)	14	core	green-blue	core-1 (inner)	cubo-octahedral	−5.7	n.a.	n.a.	937	100	0
	15 and 18a	core	green-blue	core-2 (outer)	cubo-octahedral	−4.7	−3.4	1258	824	100	0
	16	intermediate	yell.-blue	core-2 end	cubo-octahedral	−3.5	n.a.	n.a.	801	100	0
	17	intermediate	blue	cubic lobe start	cubo-octahedral	−3.1	−3.6	736	674	100	0
	18	intermediate	blue	octahedral zone	octahedral	−5.6	n.a.	n.a.	726	100	0
FG–HI (19–27, 32) via octahedral zones	19	core	blue	core-1 (inner)	cubo-octahedral	−7	−3.6	1845	810	100	0
	20	core	blue	core-2 (outer)	cubo-octahedral	−5.1	n.a.	n.a.	661	100	0
	21 and 32	intermediate	blue	intermediate	octahedral	−3.4	−3.2	1300	760	100	0
	23	intermediate	blue	intermediate	octahedral	−4.4	n.a.	n.a.	757	100	0
	24	intermediate end	blue	intermediate end	octahedral	−4.3	−2.1	561	533	100	0
	25	rim	dark	rim-1 (1st. inner)	octahedral	−3.2	1	806	131	99.9	0.1
	26	rim	blue	rim-2 (2d. inner)	octahedral	−5.6	5.3	459	194	37	63
	27	rim	dark	rim-3 (outer)	octahedral	−5.2	−3.9	788	219	37	63

Carbon and nitrogen isotope compositions and nitrogen concentrations in Yakutian diamond 1137 are considerably more systematic than in the studies mentioned above in that they vary smoothly and systematically within the core and intermediate regions. These variations are expressed by an increase in $\delta^{13}C$ and $\delta^{15}N$, and decrease of N content and aggregation away from the diamond core (Table 2, Fig. 6). In these parts of the diamond, growth occurred in a sectorial manner and the isotopic differences

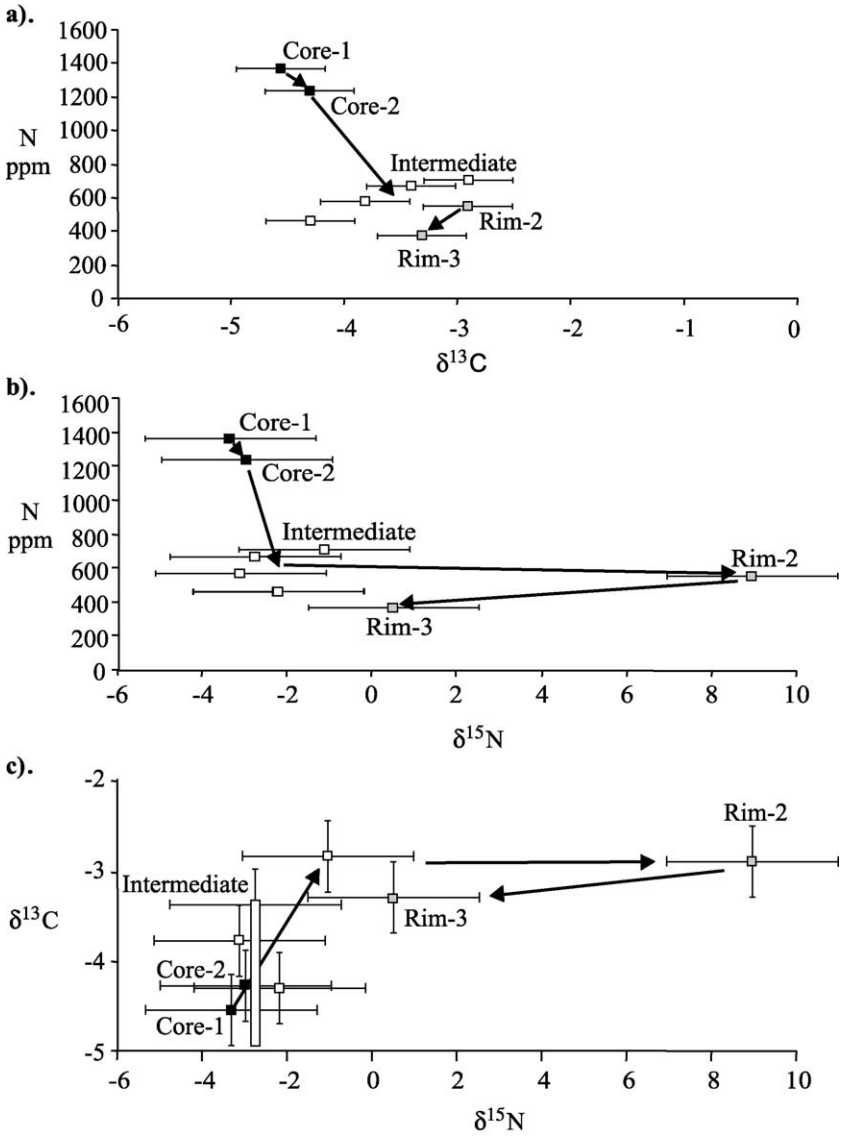

Fig. 6. Summary of general trends of nitrogen concentration, nitrogen and carbon isotopic compositions for SIMS analyses across traverses AB–AC via core of diamond plate 1137; black squares—core; white squares—intermediate; and grey squares—rim regions data. Error bars (2σ) are shown for analytical precision and are ± 0.4‰ for $\delta^{13}C$, ± 2‰ for $\delta^{15}N$, and ± 1% for N. Accuracy due to variation within the analytical standards would be an additional source of uncertainty and amounts to total estimated absolute errors of ± 0.2‰ for $\delta^{13}C$, ± 6‰ for $\delta^{15}N$, and ± 10% for N. (a) Nitrogen concentration (ppm by weight) versus $\delta^{13}C$. (b) Nitrogen concentration (ppm by weight) versus $\delta^{15}N$. (c) $\delta^{13}C$ versus $\delta^{15}N$.

could reflect those generated during the initial growth of the diamond, perhaps by a progressively evolving growth medium. The regular elemental and isotopic systematics of the central and intermediate region suggest that post-growth processes such as nitrogen aggregation or diffusion within the diamond crystal have not had any significant effects. In contrast, isotopic compositions in the rim region, in particular nitrogen isotopes, vary considerably (Fig. 6) over short distances and may be caused by different processes to those that caused the isotopic variations in the core and rim regions.

Nitrogen is the most abundant impurity in diamond and appears to behave as a compatible element because it enters the diamond lattice as single atoms isomorphously substituting for carbon atoms (Smith et al., 1959). It forms many structural defects which are responsible for diamond physical properties (Sobolev, 1978). Therefore, nitrogen should partition into the growing diamond crystal, although there is some doubt regarding the exact level of compatibility (Cartigny et al., 2001). Whether nitrogen is compatible or incompatible, its concentration can be used as an indicator of the degree of fluid remaining during diamond crystallisation if we assume that any suite of samples, or individual samples, crystallise from an evolving fluid (Hutchison et al., 1998). The decrease of N content and increase of $\delta^{13}C$ and $\delta^{15}N$ during the formation of the core and intermediate regions of diamond 1137 are suggestive of the compatible behaviour of nitrogen during continuous growth event, with isotopic fractionation occurring during crystallisation in a closed system. Deines (1980) and Deines et al. (1989) have modelled the expected relationships between nitrogen concentration and carbon isotopes for diamond growth from a mixed C–N–H–O–S vapour source under varying P–T and f_{O_2} conditions. The changing speciation of the fluid under these conditions can cause up to 4‰ variation in carbon and nitrogen isotopes over limited ranges of f_{O_2}. This is the magnitude of isotopic variation observed for the trends within the core and intermediate region of 1137 (Table 2), and hence their applicability is explored below as a possible cause of the observed variability in 1137.

Within the context of thermodynamic models (Deines, 1980; Deines et al., 1989), if we consider only carbon isotope variations, the trend to heavier carbon isotopic compositions within 1137 could be a simple reflection of the composition of a C–H–N–O fluid phase from which the diamond was possibly formed. Progressively increasing $\delta^{13}C$ values are predicted for diamond precipitation from a CO_2-rich fluid where significant amounts of the fluid are being consumed. The picture is more complicated when variations in both carbon isotope compositions and nitrogen abundance are considered. The progressive variation in carbon isotope composition towards more positive values of $\delta^{13}C$ from the core to intermediate region of 1137 might be related to fractionation factors caused by increasing f_{O_2} within the growth environment (e.g., Deines, 1980). However, such a change in $\delta^{13}C$, resulting from a change in f_{O_2}, should be accompanied by an increase in nitrogen concentration (Deines et al., 1989), and this is not observed in 1137 diamond (Fig. 6). In addition, a lowering of f_{O_2} in the growth environment should also translate into a negative correlation between $\delta^{13}C$ and $\delta^{15}N$. Such correlations are crudely defined in some diamonds from Mbuji Mayi, Zaire (Javoy et al., 1984), but are the opposite of the positive correlation observed for sample 1137 (Fig. 6). Therefore, the coupled carbon and nitrogen isotope systematics of the Core and Intermediate regions of diamond 1137 are not consistent with formation from a C–H–N–O fluid phase within the framework of the models proposed by Deines and coworkers.

The rim region of 1137 is more remarkable for the large, erratic changes observed in nitrogen isotope composition over very short length-scales (Fig. 6). Nitrogen isotopes in the rim range up to very heavy $\delta^{15}N$ values (+9‰). Such heavy nitrogen isotope compositions are generally uncommon in natural diamonds studied previously (Boyd et al., 1987; Boyd and Pillinger, 1994; Cartigny et al., 1997; 1998a,b; 1999; Deines et al., 1989; Bulanova et al., 1999). Similar heavy nitrogen isotope compositions are reported for many Argyle diamonds (van Heerden, 1993; van Heerden et al., 1995) and for some cores of coated diamonds from the Congo (Boyd et al., 1987). Recently, SIMS measurements have revealed comparably heavy nitrogen isotope compositions within other Siberian diamonds, in zones consisting of fine sub-zones of different physical types (Hauri et al., 1999). For example, an octahedral core region of eclogitic diamond 1013 (Mir pipe) displayed highly

variable nitrogen abundances (14–1153 ppm by weight) over short distances and was extremely inhomogeneous in carbon and nitrogen isotopes (Hauri et al., in press). In sample 1013, $\delta^{13}C$ in the core area varied from −8.8‰ to +1.7‰ and $\delta^{15}N$ from −12.9‰ to +5.3‰, but without any systematic correlation between the two isotope systems. In samples 1137 and 1013 studied by Hauri et al. (in press), positive $\delta^{15}N$ values appear to correlate with diamond areas composed of fine intergrowths between diamond of different physical properties. The magnitude of these isotopic variations is far greater than those expected from isotopic fractionation due to changes such as in temperature or f_{O_2} during solid–fluid equilibria.

Several alternative suggestions may explain the isotope and nitrogen concentration systematics of the rim region of 1137. Rim growth may have occurred rapidly and it is possible that isotope fractionation, in particular nitrogen, could have been affected by kinetic processes overriding thermodynamic considerations at the crystal surface, especially when nitrogen concentrations were at low levels. The most fractionated, heaviest nitrogen isotope compositions correspond to the lowest nitrogen concentrations, suggesting the possibility that kinetic effects might have been more dominant when N-bearing species were most dispersed.

Alternatively, it is possible that the sudden changes towards much heavier nitrogen isotope compositions in the rim area reflect a rapidly changing source of N-bearing species, with the isotopically heavier source being less rich in nitrogen. This nitrogen source has $\delta^{13}C$ values that are generally heavier than the canonical mantle range of −5‰ to −6‰ and has C–N isotope characteristics that could be consistent with subducted crustal nitrogen. This hypothesis cannot presently be substantiated from any other evidence. An additional possibility is that the rim region of the diamond was a much later addition and grew from fluids unrelated to those that were parental to the main diamond mass.

Finally, extreme isotopic and nitrogen abundance variations over short length-scales in sample 1137 could have resulted from post-growth processes such as nitrogen aggregation. Post-growth nitrogen aggregation is common for octahedral growth zones within diamonds, creating narrow sub-zones of 1aA and N-free (type II) diamond. In the Yakutian diamonds studied so far, nitrogen isotopes in such complex zones of differing aggregation have very variable nitrogen isotope compositions and associated heavy $\delta^{15}N$ values. This also appears to be the case for Western Australian diamonds (van Heerden, 1993; van Heerden et al., 1995).

The tendency for nitrogen atoms in the diamond lattice to aggregate upon heating into forms with much higher activation energies than single nitrogen atoms has the effect of greatly reducing diffusion rates (Harte et al., 1999) and making this process an unlikely candidate for effective isotopic fractionation. In addition, it is difficult to see why such a process should create mostly isotopically heavy regions, without the complimentary isotopically light regions being evident, unless we have not sampled them.

Almost all the carbon–nitrogen isotope values for diamond 1137 lie within the global peridotitic $\delta^{13}C$–$\delta^{15}N$ field for diamonds (Fig. 7). Cartigny et al. (2001) have recently compiled the majority of pub-

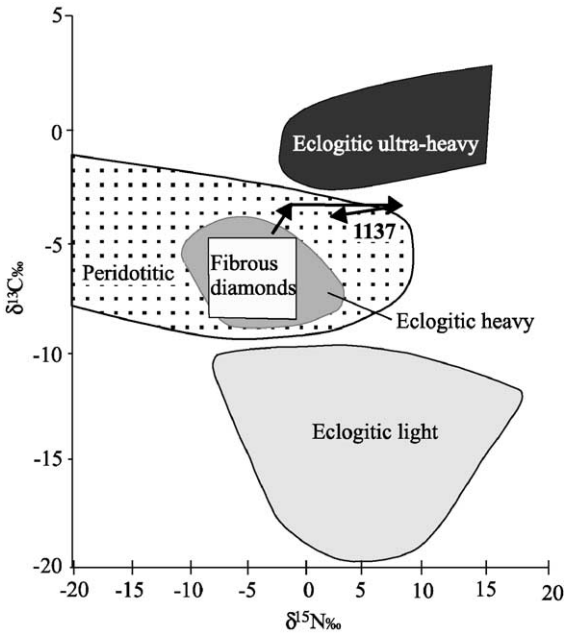

Fig. 7. General carbon and nitrogen isotopic trends for sample 1137 compared with worldwide fields for the carbon and nitrogen isotope composition of diamonds. Additional data from Boyd and Pillinger (1994), Cartigny et al. (1998a,b, 1999), Bulanova et al. (1999), and Shelkov et al. (in press).

lished data for over 1200 analyses of macro diamonds that have been investigated for both carbon isotopes and nitrogen abundance. Our examination of the relationship between $\delta^{13}C$ and nitrogen concentration for all available data (Cartigny et al., 2001) reveals that approximately 90% of diamonds are located within a restricted compositional field defining a relatively narrow carbon isotope range, within which the 1137 trend lies (Fig. 8). This predominant relationship between $\delta^{13}C$ and nitrogen concentration is largely composed of peridotitic diamonds with some isotopically heavy eclogitic and fibrous diamonds (Fig. 7). Cartigny et al. (2001) proposed that individual suites contain diamond populations showing subvertical trends of varying N-abundance at constant $\delta^{13}C$ resulting from kinetic processes related to very slow diamond growth (''slow growth fractionation'' in Cartigny et al.'s, 2001 terminology). Data for sample 1137 follow this same pattern, but although the decrease in nitrogen abundance is by a factor of 4 and covers approximately 1/3 of the total range of N variation in the worlds' diamonds, there is a very subtle change in carbon isotopes to slightly heavier compositions (Fig. 8). We tentatively suggest that this trend might be representative of the slow carbon fractionation for diamonds growing from CO_2-bearing mantle melts/fluids.

5.3. Comparison to synthetic diamond

From the measurements made so far, there appears to be no significant or consistent fractionation of carbon or nitrogen isotopes between the cubic and octahedral growth sectors of this natural diamond. Such observation contrasts with the marked difference in nitrogen isotope composition observed between the cubic and octahedral growth sectors of a synthetic diamond by Boyd et al. (1988).

The isotopic fractionation measured in synthetic diamonds can be readily explained by the dramatic differences in the processes of diamond growth in nature compared with high $P-T$ experiments. In natural diamonds, cuboid growth in the stability region where octahedral faces are stable is characterised by unfaceted/hummocky growth. In contrast, synthetic diamonds exhibit true cubic (faceted/tangential) growth (Pal'yanov et al., 1997). The development of habit in synthetic diamonds is controlled by the relative surface free energies of the cubic and octahedral faces, which is a function of $P-T$. It is possible that the difference in surface free energies causes the marked fractionation observed in synthetic diamonds (Boyd et al., 1988), but this effect is absent during diamond growth in nature because true cubic faces never develop. The lack of significant and systematic

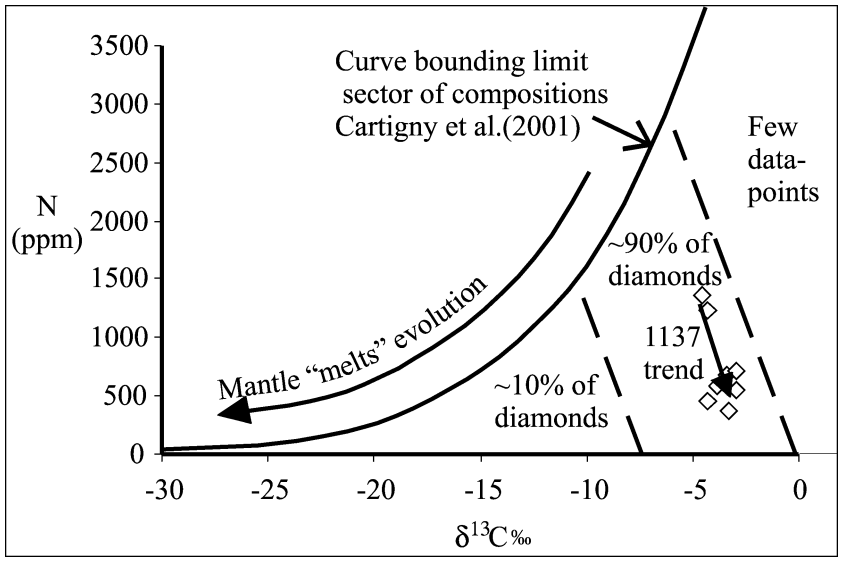

Fig. 8. Carbon isotope and nitrogen abundance trend for sample 1137 compared to worldwide data summarised by Cartigny et al. (2001).

carbon or nitrogen isotopic fractionation in the sector-growth diamond studied here provides further support for a surface-free energy effect controlling isotopic fractionation in synthetic diamonds.

6. Conclusions

We have performed the first comprehensive study of the carbon and nitrogen isotopic systematics of a natural diamond with sectorial growth. The sample has a graphite "seed" inclusion enriched in K, Ca, Ti, Rb, and Sr, which suggests the diamond may have grown from a carbonate melt/fluid interacting with upper mantle rocks.

Distinctive isotopic trends have been found, expressed by an increase in $\delta^{13}C$ and $\delta^{15}N$ values and a decrease of nitrogen concentrations and nitrogen aggregation from the core region towards the intermediate zones of the diamond. The formation of the mixed-habit growth sectors, comprising the core and intermediate regions of the diamond, most likely took place during a continuous event with progressive isotopic fractionation of carbon and nitrogen accompanied by cooling. The progressive trends in nitrogen concentration and aggregation, in addition to those shown by carbon and nitrogen isotopes within the sectorial core and intermediate areas of 1137, are believed to reflect diamond growth from an evolving fluid medium.

The isotopic trends in the core-intermediate regions of 1137 differ from the trends of decreasing $\delta^{13}C$ and increasing $\delta^{15}N$, which are suggested to arise from isotopic fractionation during diamond growth in certain other diamond suites described by Cartigny et al. (1998a). Neither are the trends predicted from thermodynamic modelling of fluid–solid equilibria in a C–N–O–H-bearing system due to changes in parameters such as f_{O_2} (Deines, 1980; Deines et al., 1989). The origin of the isotopic variations observed within 1137 diamond is therefore difficult to explain in the frame of existing models.

Within the rim region of 1137, where growth was entirely octahedral, there are more dramatic and non-systematic variations in nitrogen abundance, nitrogen aggregation, and nitrogen isotopic compositions. Several explanations may exist for these phenomena, including kinetic effects during growth of the rim diamond under different conditions from those of the core-intermediate regions, rapidly changing fluid sources during diamond growth, or growth of the rim during a later event, from a different fluid source.

Harte et al. (1999) have argued that diffusion processes within some diamonds have affected their carbon isotope compositions as a result of storage at mantle temperatures over billion-year time scales. The isotopic variations recorded by this and other Yakutian diamonds (Hauri et al., 1999), some having mantle residence times estimated at c. 3 Ga (Pearson et al., 1999), indicate that diffusion has not eradicated isotopic signatures reflecting processes operating during diamond growth. This may suggest a different thermal history between diamonds from Yakutia and other cratonic areas such as the Kaapvaal craton. In this regard, thermobarometry estimates of the geotherm beneath the Siberian craton indicate that it may be anomalously cool compared to other cratons such as Kaapvaal (Griffin et al., 1991).

Measurements made in this study of a natural sectorially zoned diamond reveal no significant or consistent fractionation of carbon or nitrogen isotopes between the cubic and octahedral growth sectors. Such contrasts with marked difference in nitrogen isotope composition between the cubic and octahedral growth sectors of a synthetic diamond were observed by Boyd et al. (1988). We ascribe these variations to differences between the processes of diamond growth in nature compared with high $P–T$ experiments.

Further work is needed to establish if the results obtained for diamond 1137 are typical for the Yakutian diamond population. The significant within-diamond isotopic variations found in 1137 and other Siberian diamonds (Hauri et al., 1999; Bulanova et al., 1999), together with those evident in the diamonds described by Harte et al. (1999) and Fitzsimons et al. (1999), illustrate the potential and the need for in-situ carbon and nitrogen isotopic measurements if we are to identify the growth media and conditions of diamonds worldwide.

Acknowledgements

The authors are indebted to Professor A. Lang and Judith Milledge for their fruitful discussions and help throughout writing of the paper. We are grossly in-

debted to Chris B. Smith for contributing much towards the development of this paper, for spotting numerous inconsistencies, and for generally keeping us on track. Jinghua Zhang assisted with the ion probe technique development and measurements. P. Cartigny and S. Boyd are thanked for most helpful reviews. We acknowledge the foresight of V. Beskrovanov who recognised the special nature of sample 1137 and highlighted the need for further study.

This research has been supported by The Royal Society Grant RSG 21948, UK. **[RR]**

References

Beskrovanov, V.V., 1992. Ontogeniya of Diamond Nauka, Novosibirsk, 165 pp. (in Russian).

Boyd, S.R., Pillinger, C.T., 1994. A preliminary study of 15N/14N in octahedral growth form diamonds. Chem. Geol. 116, 43–59.

Boyd, S.R., Mattey, D.P., Pillinger, C.T., Milledge, H.J., Mendelssohn, M., Seal, M., 1987. Multiple growth events during diamond genesis: an integrated study of carbon and nitrogen isotopes and nitrogen aggregation state in coated stones. Earth Planet. Sci. Lett. 86, 341–353.

Boyd, S.R., Pillinger, C.T., Milledge, H.J., Mendelssohn, M.J., Seal, M., 1988. Fractionation of nitrogen isotopes in a synthetic diamond of mixed crystal habit. Nature 331, 604–607.

Boyd, S.R., Pillinger, C.T., Milledge, H.J., Mendelssohn, M.J., Seal, M., 1992. C and N isotopic composition and the infrared absorption spectra of coated diamonds: evidence for the regional uniformity of CO_2-H_2O fluids in lithospheric mantle. Earth Planet. Sci. Lett. 109, 633–644.

Bulanova, G.P., 1995. The formation of diamond. J. Geochem. Explor. 53, 1–23.

Bulanova, G.P., Varshavsky, A.V., Leskova, N.V., Nikishova, L.V., 1979. About central inclusions in natural diamonds. Docladi Academii Nauk USSR, 244, N3, 704–706.

Bulanova, G.P., Varshavsky, A.V., Leskova, N.V., Nikishova, L.V., 1986. Central inclusions as indicators of growth conditions of natural diamond. Physical Properties and Mineralogy of Diamond, Institute of Geology, Yakutian Branch of Russian Academy of Sciences, Yakutsk, pp. 29–45 (in Russian).

Bulanova, G.P., Griffin, W.L., Ryan, C.G., 1998. Nucleation environment of diamonds from Yakutian kimberlites. Min. Mag. 62 (3), 409–419.

Bulanova, G.P., Shelkov, D., Milledge, H.J., Hauri, E.H., Smith, B.C., Chris, B., 1999. Nature of eclogitic diamonds from Yakutian kimberlites: evidence from isotopic composition and chemistry of inclusions. Proc. 7th Int. Kimberlite Conf., vol. 1. Red Roof Design, Cape Town, pp. 57–65.

Cartigny, P., Boyd, S.R., Harris, J.W., Javoy, M., 1997. Nitrogen isotopes in peridotitic diamonds from Fuxian, China: the mantle signature. Terra Nova 9, 175–179.

Cartigny, P., Harris, J.W., Javoy, M., 1998a. Eclogitic diamond formation at Jwaneng: no room for recycled component. Science 280, 1421–1424.

Cartigny, P., Harris, J.W., Phillips, D., Girard, M., Javoy, M., 1998b. Subduction-related diamonds? The evidence for a mantle derived origin from coupled $\delta^{13}C-\delta^{15}N$ determinations. Chem. Geol. 147, 147–159.

Cartigny, P., Harris, J.W., Javoy, M., 1999. Eclogitic, peridotitic and metamorphic diamonds and the problems of carbon recycling—the case of Orapa (Botswana). Proc. 7th Int. Kimberlite Conf., vol. 1. Red Roof Design, Cape Town, pp. 117–124.

Cartigny, P., Harris, J.W., Javoy, M., 2001. Diamond genesis, mantle fractionation and mantle nitrogen content: a study of $\delta^{13}C-N$ concentrations in diamonds. Earth Planet. Sci. Lett. 185, 85–98.

Deines, P., 1980. The carbon isotopic composition of diamonds: relationship to diamond shape, color, occurrences and vapour composition. Geochim. Cosmochim. Acta 44, 943–961.

Deines, P., Harris, J.W., Spear, P.M., Gurney, J.J., 1989. Nitrogen and $\delta^{13}C$ content of Finch and Premier diamonds and their implications. Geochim. Cosmochim. Acta 53, 1367–1378.

Evans, T., Harris, J.W., 1989. Nitrogen aggregation, inclusion equilibration temperatures and the age of diamonds. In: Ross, J. (Ed.), Kimberlites and Related Rocks, Vol. 2, Their Mantle/Crust Setting, Diamonds, and Diamond Exploration. Proc. Fourth International Kimberlite Conference, Perth. Geol. Soc. Aust., Spec. Publ., vol. 14, pp. 1001–1006.

Fitzsimons, I.C.W., Harte, B., Chinn, J.J., Gurney, J.J., Taylor, W.R., 1999. Extreme chemical variation in complex diamonds from George Creek, Colorado: a SIMS study of carbon isotope composition and nitrogen abundance. Min. Mag. 63 (6), 857–878.

Galimov, E.M., 1984. Variations of carbon isotope composition and their relation with diamond growth conditions. Geochemistry 8, 1091–1118.

Galimov, E.M., 1991. Isotope fractionation related to kimberlite magmatism and diamond formation. Geochim. Cosmochim. Acta 55, 1697–1708.

Griffin, W.L., Gurney, J.J., Sobolev, N.V., Ryan, C.G., 1991. Comparative geochemical evolution of cratonic lithosphere: south Africa and Siberia. Ext. Abstr., 5th Int. Kimberlite Conf., Araxa, Brasilia. CPRM Spec. Publ., vol. 2/91, pp. 119–121.

Griffin, B.J., Bulanova, G.P., Taylor, W.R., 1995. CL and FTIR mapping of nitrogen content and hydrogen distribution in a diamond from the Mir pipe—constraints on growth history. Ext. Abstr. 6th Int. Kimberlite Conf., United Institute of Geology, Geophysics and Mineralogy, Novosibirsk, pp. 191–193.

Harte, B., Otter, M.L., 1992. Carbon isotope measurements on diamonds. Chem. Geol. 101, 177–183.

Harte, B., Fitzsimons, C.W., Harris, J.W., Otter, M.L., 1999. Carbon isotope ratios and nitrogen abundances in relation to cathodoluminescence characteristics for some diamonds from Kaapvaal province, S. Africa. Min. Mag. 63 (6), 829–856.

Hauri, E.H., Pearson, D.G., Bulanova, G.P., Milledge, H.J., 1999. Microscale variations in C and N isotopes within mantle diamonds revealed by SIMS. Proc. 7th Int., Kimberlite Conf., vol. 1. Red Roof Design, Cape Town, pp. 341–347.

Hauri, E.H., Wang, J., Pearson, D.G., Bulanova, G.P., in press. Microanalysis of $\delta^{13}C$, $\delta^{15}N$ and N abundances in diamonds by secondary ion mass spectrometry (SIMS). Chem. Geol.

Hutchison, M.T., Cartigny, P., Harris, J.W., 1998. Carbon and nitrogen compositions and cathodoluminescence characteristics of transitional zone and lower mantle diamonds from Sao Luiz, Brazil. Extended Abstracts, 7th Int. Kimberlite Conf., Cape Town, 336–338.

Javoy, M., 1997. The major volatiles of the Earth: their origin, behaviour and fate. Geophys. Res. Lett. 24, 177–180.

Javoy, M., Pineau, F., Demaiffe, D., 1984. Nitrogen and carbon isotopic composition in the diamonds of Mbuji Mayi (Zaire). Earth Planet. Sci. Lett. 68, 399–412.

Javoy, M., Pineau, F., Delorme, H., 1986. Carbon and nitrogen isotopes in the mantle. Chem. Geol. 57, 41–62.

Kirkley, M.B., Gurney, J.J., Otter, M.L., Hill, S.J., Daniels, L.R.M., 1991. The application of C isotope measurements to the identification of the sources of C in diamonds, a review. Appl. Geochem. 6, 477–494.

Mendelssohn, M.J., Milledge, H.J., 1995. Geologically significant information from routine analysis of the mid-infrared spectra of diamonds. Int. Geol. Rev. 37, 95–110.

Moore, M., 1985. Diamond morphology. Ind. Diamond Rev. 2, 67–71.

Moore, M., Lang, A.R., 1972. On the internal structure of natural diamonds of cubic habit. Phila. Mag. 26 (6), 1313–1326.

Navon, O., 1999. Diamond formation in the Earth's mantle. Proc. 7th Int. Kimberlite Conf., vol. 2. Red Roof Design, Cape Town, pp. 584–604.

Pal'yanov, Yu.N., Khokhryakov, A.F., Borzdov, Yu.M., Sokol, A.G., Gusev, V.A., Rylov, G.M., Sobolev, N.V., 1997. Growth conditions and real structure of synthetic diamond crystals. Russ. Geol. Geophys. 38 (5), 245–920.

Pearson, D.G., Shirey, S.B., Bulanova, G.P., Carlson, R.W., Milledge, H.J., 1999. Re–Os isotope measurements of single sulphide inclusions in Siberian diamond and its nitrogen aggregation systematics. Geochim. Cosmochim. Acta 63 (5), 703–711.

Shelkov, D., Verchovsky, A.B., Milledge, H.J., Bulanova, G.P., Taylor, W., Pillinger, C.T., in press. Carbon and nitrogen isotopic composition of mantle diamonds and their application for the earth's evolution model.

Smith, W.V., Gelles, S.L., Sorokin, P.P., 1959. Electron spin resonance of acceptor states in diamond. Phys. Rev. 115 (6), 1546–1552.

Sobolev, E.V., 1978. Nitrogen Centres and Growth of Natural Diamond Crystals. The Problems of Petrology of the Earth Crust and the Upper Mantle. Nauka, Novosibirsk, pp. 245–255 (in Russian).

Suzuki, S., Lang, A.R., 1976. Internal Structure of Natural Diamonds Revealing Mixed-Habit Growth. Diamond Research, Ind. Diamond Inform. Bureau, London, pp. 39–47.

Swart, P.K., Pillinger, C.T., Milledge, H.J., Seal, M., 1983. Carbon isotopic variation within individual diamonds. Nature 303, 793–795.

Taylor, W.R., Jaques, A.L., Ridd, M., 1990. Nitrogen defect aggregation characteristics of some Australian diamonds: time–temperature constraints on the source regions of pipe and alluvial diamonds. Am. Mineral. 75, 1290–1310.

Taylor, W.R., Canil, D., Milledge, H.J., 1996. Kinetics of Ib to IaA nitrogen aggregation in diamond. Geochim. Cosmochim. Acta 60, 4725–4733.

van Heerden, L.A., 1993. A nitrogen and carbon stable isotope study of some Western Australian diamonds. PhD thesis, Open University, Milton Keynes, UK.

van Heerden, L.A., Boyd, S.R., Milledge, H.J., Pillinger, C.T., 1995. The carbon and nitrogen isotope characteristics of the Argyle and Ellendale diamonds, Western Australia. Int. Geol. Rev. 37, 39–50.

Varshavsky, A.V., 1968. Anomalous Birefringence and Internal Morphology of Diamonds Nauka, Moscow, 89 pp. (In Russian).

Wilding, M.C., Harte, B., 1990. Carbon isotope variation in a zoned Bultfontein diamond determined by SIMS. Geol. Soc. Austs. Abstr. 27, 112.